



Dye removal and kinetics of adsorption by magnetic chitosan nanoparticles

Fatemeh Hosseini^a, Somayeh Sadighian^{b,*}, Hassan Hosseini-Monfared^a,
Niyaz Mohammad Mahmoodi^c

^aFaculty of Science, Department of Chemistry, University of Zanjan, Zanjan, Iran

^bDepartment of Pharmaceutical Biomaterials, School of Pharmacy, Zanjan University of Medical Sciences, 45139-56184 Zanjan, Iran, Tel. +98 24 33473638; Fax: +98 24 33473639; email: sadighian@zums.ac.ir

^cDepartment of Environmental Research, Institute for Color Science and Technology, Tehran, Iran

Received 6 April 2015; Accepted 5 January 2016

ABSTRACT

Treatment and recycle of wastewater provide a route to water shortage in the world. Dyes are one of the contaminant in the environment. In this study, magnetic chitosan nanocomposites were fabricated through a facile chemical route and their dye removal ability as an adsorbent were studied. Fourier transform infrared spectroscopy, X-ray diffraction, and scanning electron microscopy were used to characterize the synthesized nanosorbents. The results showed that the synthesized adsorbents possess quite a good adsorption capacity (with maximum adsorption capacity of 20.5 mg/g by pseudo-second-order model) to dye due to the abundant amino and hydroxyl groups of chitosan. In addition, they can be easily and rapidly extracted from water by magnetic force, and showed good reusability in regeneration studies. The magnetic chitosan nanocomposites could be recovered conveniently and possessed of excellent adsorptive property; it can be developed as an economical and alternative adsorbent to treat dye wastewater.

Keywords: Magnetic chitosan nanocomposite; Synthesis; Dye removal; Kinetic

1. Introduction

Modern industrial activities and households generate a lot of wastewater each year. Treatment and recycle of wastewater provide a route to water shortage in the world [1]. There are many types of pollutant presented in wastewater. Dyes are one of the contaminant in the environment. Nowadays, these compounds widely used for a long time in many industrial fields, such as paper making, coating and textiles, leather, cosmetics, ink [2,3] to color their products. A great range of methods has been

developed for the removal of synthetic dyes from wastewater to decrease their trace on the environment, such as adsorption [4], chemical oxidation [5], microbiological or enzymatic decomposition [6], liquid–liquid extraction [7]. Adsorption technique is proved to be an attractive process for the treatment of dye-bearing wastewaters with no unwanted byproducts [1]. The variety of dye adsorbents including activated carbons (granular or powder) [8], graphene [9], polymeric materials [10], because of their large surface area, high-adsorption capacity, have been used to remove dyes from wastewater. Recently, a unrivaled magnetic carrier technology based on the magnetic materials has been reported by several

*Corresponding author.

groups [2,11–13]. Magnetite (Fe_3O_4) and maghemite ($\gamma\text{-Fe}_2\text{O}_3$) have been widely used as magnetic material because of their privileged magnetic properties, chemical stability, and biocompatibility [14–17]. Magnetic nanoparticles are proper for removal of dye from lake and river, because it can be recollected from water comfortably [18,19]. Magnetite nanoparticles desire to aggregate due to strong magnetic dipole–dipole gravitation between nanoparticles. So, stabilizers such as surfactants, metal nanoparticles [20], and polymeric compounds [21] with some specific functional groups are used to modify these nanoparticles to increase the stability. Conventional magnetic adsorbents are generally commercial carriers made of magnetite nanoparticles modified with polymers [22] in which suitable functional groups are present on the adsorbent surface. Chitosan is a suitable biopolymer used in order to remove dyes and metal ions from aqueous solution, because of its high-adsorption capacities and low-cost materials obtained from natural resources and the preparations of magnetic chitosan beads are of great interest [23–25]. Chitosan, poly(1–4)-2-amino-2-deoxy-d-glucan, the second most plenty biopolymer in nature after cellulose, has attracted great attention due to its low cost and non-toxicity. Chitosan has two types of reactive functional groups, amino groups, and hydroxyl groups. Due to its inherent specifications, the natural polymer is often chosen as an efficient adsorbent for the removal or the recovery of hazardous dyes and heavy metals [4]. Giri et al. prepared magnetite nanoparticles to adsorb methyleneblue (cationic) and Congo red (anionic) dyes [26]. Piccin et al. investigated the application of chitosan for removal of food dye FD&C Red 40 [22]. Zhu et al. used $\gamma\text{-Fe}_2\text{O}_3$ -chitosan nanoparticles to adsorb methyl orange (MO) [2,27]. Shen and co-workers investigated the application of magnetic chitosan-Fe(III) hydrogel for removal of C.I. Acid Red 73 [12].

In this work, we reported the synthesis of three magnetic dye adsorbents based on the Fe_3O_4 -chitosan nanoparticles with two types of cross linkers (sodium tripolyphosphate and glutaraldehyde) to compare the kinetic and amount of dye adsorption. The magnetic core can provide a convenient platform for the facile separation and the chitosan shell can prevent efficiently the aggregation and chemical decomposition of Fe_3O_4 in a rough environment. This type of magnetic adsorbent, featuring good compatibility, low cost, easy and rapid extraction/regeneration, and handy operation which may be useful for further research and practical applications for dye removal.

2. Experimental

2.1. Materials and methods

Ferric chloride hexahydrate ($\text{FeCl}_3 \cdot 6\text{H}_2\text{O}$), ferrous chloride tetrahydrate ($\text{FeCl}_2 \cdot 4\text{H}_2\text{O}$), sodium tripolyphosphate (TPP), glutaraldehyde, glacial acetic acid, and MO were from Merck and purchased locally. Chitosan of molecular weight in the range of 10^5 – 3×10^5 g/mol and degree of deacetylation $\geq 75\%$ was obtained from Sigma.

2.2. Preparation of Fe_3O_4 -chitosan nanoparticles

Magnetic Fe_3O_4 -chitosan nanoparticles were prepared by chemical co-precipitation of ferrous chloride and ferric chloride with NH_3 in the presence of chitosan followed by treatment under the mechanical stirring [28]. Briefly, iron(II) chloride (1 mmol) and iron (III) chloride (2 mmol) were dissolved in acetic acid solution of chitosan and the resulting solution was chemically precipitated at 80°C by adding into 30% NaOH solution under the mechanical stirring, at a controlled pH (10). The dark brown product was separated by an external magnet and washed three times with distilled water and dried in vacuum conditions at 60°C for 12 h.

2.3. Preparation of Fe_3O_4 -chitosan-TPP nanoparticles

Fe_3O_4 -chitosan-TPP nanogels were created by modified ionic gelation with negatively charged TPP ions and positively charged chitosan [28]. The solution of TPP (5 mL, 0.1% (w/v)) was added to final product of Section 2.2, and then stirred mechanically for 15 min. The magnetic nanoparticles were separated by an external magnet and washed several times with distilled water and dried at 60°C for 12 h.

2.4. Preparation of Fe_3O_4 -chitosan-glutaraldehyde nanoparticles

Fe_3O_4 -chitosan-glutaraldehyde nanogels were prepared by cross linking between them. Glutaraldehyde was added to chitosan solution to initiate the reaction between the amino groups of chitosan and the aldehyde groups of glutaraldehyde. One milliliters of glutaraldehyde was added to final product of Section 2.2, and then stirred mechanically for 15 min. The product was separated by an external magnet and washed several times with distilled water and dried at 60°C for 12 h.

2.5. Adsorption experiments

The adsorption of dye from aqueous solutions by magnetic nanoparticles was studied as follows. The adsorption of dye was evaluated by adding different concentration of adsorbent/dye solution. After the agitation at a rate of 100 rpm for 30 min under 25°C, the solution was centrifuged and small amounts of the liquid were taken to be analyzed. Methylorange concentration in supernatant after magnetic separation was monitored by UV–vis spectrophotometer at $\lambda_{\max} = 465$ nm. The amount of adsorbed dye, q_t , was calculated by Eqs. (1) and (2):

$$q_t = (C_0 - C)V/W \quad (1)$$

$$E = (C_0 - C)/C_0 \times 100\% \quad (2)$$

where q_t is the dye capacity in the sorbent at equilibrium (mg/g), C_0 is the initial dye concentration in the liquid-phase (mg/L), C is instantaneous dye concentration at time t (mg/L), V is the volume of solution (L), and W is weight of the adsorbent used (g).

2.6. Regeneration and reuse experiments

Regeneration of the adsorbents was carried out via desorption of MO from nanogels. Desorption of MO dye molecules from three types of nanogel was carried out using 50 mg adsorbent in 500 ml of 0.1 M NaOH solution (elution medium) for 48 h. After being shaken at temperature $24 \pm 1^\circ\text{C}$, and 200 rpm in a shaker, the nanogels were taken out and then dried at 60°C for 24 h.

2.7. Characterization of synthesized nanoparticles

Crystal structures of samples were determined by performing X-ray diffraction (XRD) on Bruker D8 Advance XRD spectrometer with a Cu K_α radiation (0.154060 nm) and the voltage 40 kV and current 30 mA. Nanostructures of samples were observed by scanning electron microscopy (SEM) with a Hitachi f4160 machine (Tokyo, Japan). Fourier transform infrared (FT-IR) spectra of nanoparticles were measured with a Matson FT-IR spectrophotometer in the range of 400–4,000 cm^{-1} as KBr disks at room temperature. The hydrodynamic diameter of the nanoparticles was measured using the Zetasizer Nano-ZS3600 (Malvern Instruments, Malvern, UK) dynamic light scattering (DLS) with the sonicated nanoparticles in water before measurement.

3. Results and discussion

3.1. Characterization of magnetic nanoparticles

3.1.1. XRD analysis

XRD is an effective method to study the entity of intercalation in composites. XRD patterns of magnetite (Fe_3O_4) nanoparticles are shown in Fig. 1. Diffraction peaks of magnetite nanoparticles at 2θ of 18.2°, 30.0°, 35.5°, 42.9°, 53.6°, 57.2°, and 63° corresponded to (1 1 1), (2 2 0), (3 1 1), (4 0 0), (4 2 2), (5 1 1), and (4 4 0) lattice planes of Fe_3O_4 (Fig. 1) which was consistent with the database of magnetite (Fe_3O_4) [29,30]. In all curves, diffraction peaks can be indexed to face-centered cubic structure of magnetite. The intensities of Fe_3O_4 -nanoparticles diffraction peaks for nanogels core-shell were weaker than those of the Fe_3O_4 -chitosan nanoparticles, which indicate the presence of gel materials on the surface of Fe_3O_4 nanoparticles.

3.1.2. Magnetic properties

The magnetic properties of nanoparticles are prepared by vibrating sample magnetometer (VSM). Fig. 2. shows the magnetization curves of three types of Fe_3O_4 -chitosan nanoparticles. The results showed that all samples exhibited superparamagnetic properties. The saturation magnetization values (M_s) of the Fe_3O_4 -chitosan nanoparticles, Fe_3O_4 -chitosan-TPP nanogels, and Fe_3O_4 -chitosan-glutaraldehyde nanogels were 73, 66, and 58 emu/g at 9,000 Oe, respectively. These values are although strong enough for a convenient magnetic separation [31].

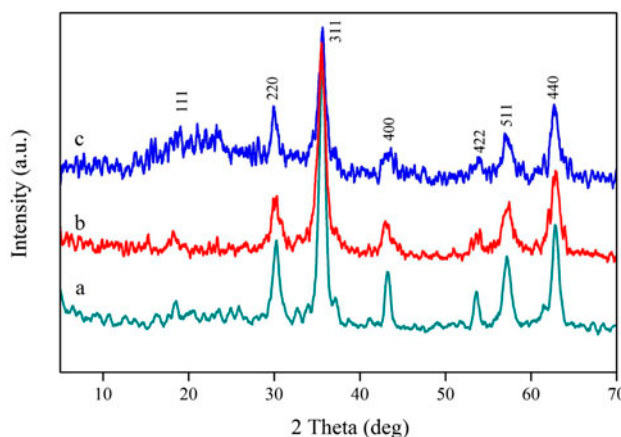


Fig. 1. XRD patterns of the (a) Fe_3O_4 -chitosan nanoparticles, (b) Fe_3O_4 -chitosan-TPP nanogels, and (c) Fe_3O_4 -chitosan-glutaraldehyde nanogels.

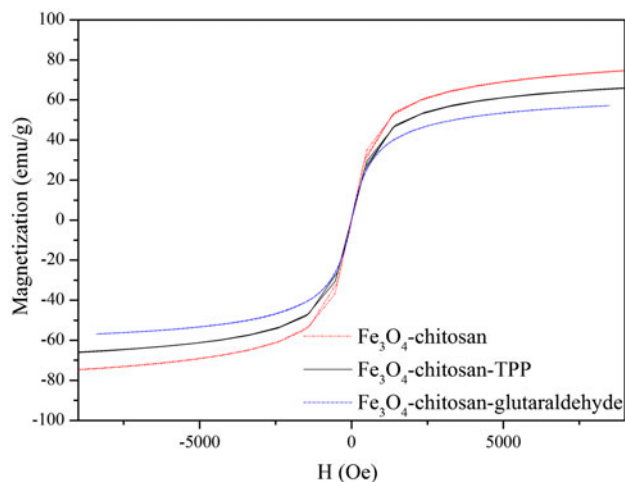


Fig. 2. Magnetization curves obtained by VSM at room temperature.

3.1.3. Fourier transform infrared spectroscopy analysis

The characteristic peak of Fe_3O_4 at 578 cm^{-1} could be observed in all of the three curves which demonstrated that all synthesized nanoparticles were Fe_3O_4 . From (b), the characteristic peaks of chitosan could be observed. The band of $1,615\text{ cm}^{-1}$ was assigned to N–H bending vibration and the peak of $1,381\text{ cm}^{-1}$ to C–O stretching of primary alcoholic group in chitosan [32]. The results suggested the integration of Fe_3O_4 nanoparticles and chitosan in the Fe_3O_4 -chitosan nanoparticles. In Fe_3O_4 -chitosan-TPP nanogels (c), the bands at $2,922$, $2,845$, and $1,405\text{ cm}^{-1}$ represent the presence of –CH and – CH_2 groups. The bands at $1,070$ and $1,100\text{ cm}^{-1}$ are attributed to the $\nu(\text{C}=\text{O})$ of chitosan and $\nu(\text{P}=\text{O})$ of TPP, respectively. The broad band at $\sim 3,420\text{ cm}^{-1}$ corresponds to the stretching vibration of – NH_3^+ and –OH groups can be related to the hydrogen bonding between chitosan and TPP. In Fe_3O_4 -chitosan-glutaraldehyde nanogels, cross linking of chitosan with glutaraldehyde takes place between NH_2 functional group of chitosan and CHO functional group of glutaraldehyde with the removal of H_2O molecule. The Fourier transform infrared spectroscopy (FT-IR) spectra of the magnetic chitosan-glutaraldehyde nanogels showed that the characteristic absorption bands appeared at 578 and $2,850\text{ cm}^{-1}$, which corresponded to Fe–O bond of Fe_3O_4 and aldehyde groups, respectively. The adsorption peaks of the magnetic chitosan-glutaraldehyde nanogels at $1,061$ and $1,126\text{ cm}^{-1}$ (C–N bond), $1,386\text{ cm}^{-1}$ (C–O stretching of primary alcoholic group), $1,610\text{ cm}^{-1}$ (– NH_2 in amide group), and $3,420\text{ cm}^{-1}$ (N–H bond) can also be observed. The results of FT-IR spectra indicated that

the magnetic chitosan were cross linked by glutaraldehyde successfully [33] (Fig. 3).

3.1.4. Particle sizes measurements

The values of hydrodynamic diameter for magnetic nanoparticles measured with DLS in distilled water are summarized in Table 1. It shows the average particle diameter (nm) and the polydispersity index (PDI) of the prepared nanoparticles. Particle size distribution curves exhibit only one peak with a small PDI indicating the low extent of magnetic nanoparticles aggregation in solutions. The hydrodynamic diameter of the particles is approximately larger than that measured with SEM. This difference may be due to the particles solvation and dynamic association in the liquid.

3.1.5. Morphological characterization

SEM provides very useful information about the particle size and polydispersity profile. Fig. 4 shows the SEM micrograph of magnetic nanoparticles. The SEM analysis of the products provides information on the size and morphology of them. Fig. 4(A) illustrates that the Fe_3O_4 -chitosan nanoparticles have uniform sphere size in a disordered distribution (with the average size of 40 nm). The morphology of Fe_3O_4 -chitosan-TPP and glutaraldehyde nanogels shows also spherical nanoparticles with uniform particle size, 26 and 18 nm , respectively (Fig. 4(B) and (C)). The particle size of Fe_3O_4 -chitosan was bigger than that of magnetic nanogels, indicating that magnetic nanogels

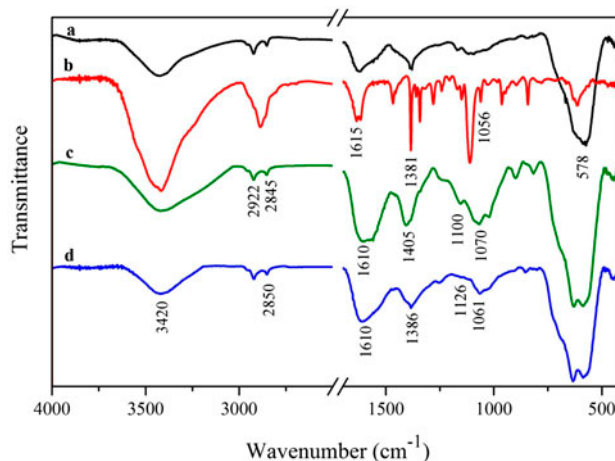


Fig. 3. FT-IR spectra of (a) Fe_3O_4 , (b) Fe_3O_4 -chitosan, (c) Fe_3O_4 -chitosan-TPP nanogels, and (d) Fe_3O_4 -chitosan-glutaraldehyde nanogels.

Table 1

Average particle diameter and polydispersion index of magnetic nanoparticles

Nanoparticles	Z-average (nm)	PDI ^a
Fe ₃ O ₄ -chitosan	78.82	0.126
Fe ₃ O ₄ -chitosan-TPP	68.74	0.266
Fe ₃ O ₄ -chitosan-Glutaraldehyde	55.93	0.165

^aPolydispersity index.

have been encapsulated by chitosan and cross linking agents (TPP and glutaraldehyde).

3.2. Effect of initial concentration on adsorption

Adsorbent samples (5, 10, and 20 mg) were added to flasks containing 10 mL of MO solution of concentration 5 mg/L. The experimental results are shown in Fig. 5. The adsorption accelerated greatly with increasing amounts of adsorbent. When 20 mg of all of three adsorbents were used, it took less than 20 min to reach adsorptions equilibrium. Eventually, equilibrium was reached and MO removal then gradually increased with increasing amounts of adsorbents.

3.3. Effect of pH on dye removal

The pH is the most important factor in affecting the adsorption process. The solution pH is one of the dominant parameters affecting the adsorption of organic dyes onto solid polymeric adsorbent [34]. The solution pH can affect the surface charge of the nano adsorbent and the dissociation of functional groups on the active sites of the adsorbent as well as the structure of the dye molecule. The effect of pH on MO adsorption was remarkable in our experimental conditions. The effects of initial solution pH on the adsorption of MO onto three nanoparticles (20 mg) were investigated at pH 4–12, 25°C, and an initial MO concentration of 5 µg/ml. Chitosan has a positively charged surface below pH 5. In acidic solution, hydrogen atoms (H⁺) in solution can protonate amine groups (–NH₂) of chitosan. As a result, the electrostatic interactions between MO anions and chitosan with positively charged surface increased in acidic solution (Fig. 6).

3.4. Kinetics study of dye removal

The kinetic parameters, which are helpful for the prediction of the adsorption rate, give important information for designing and modeling the adsorption

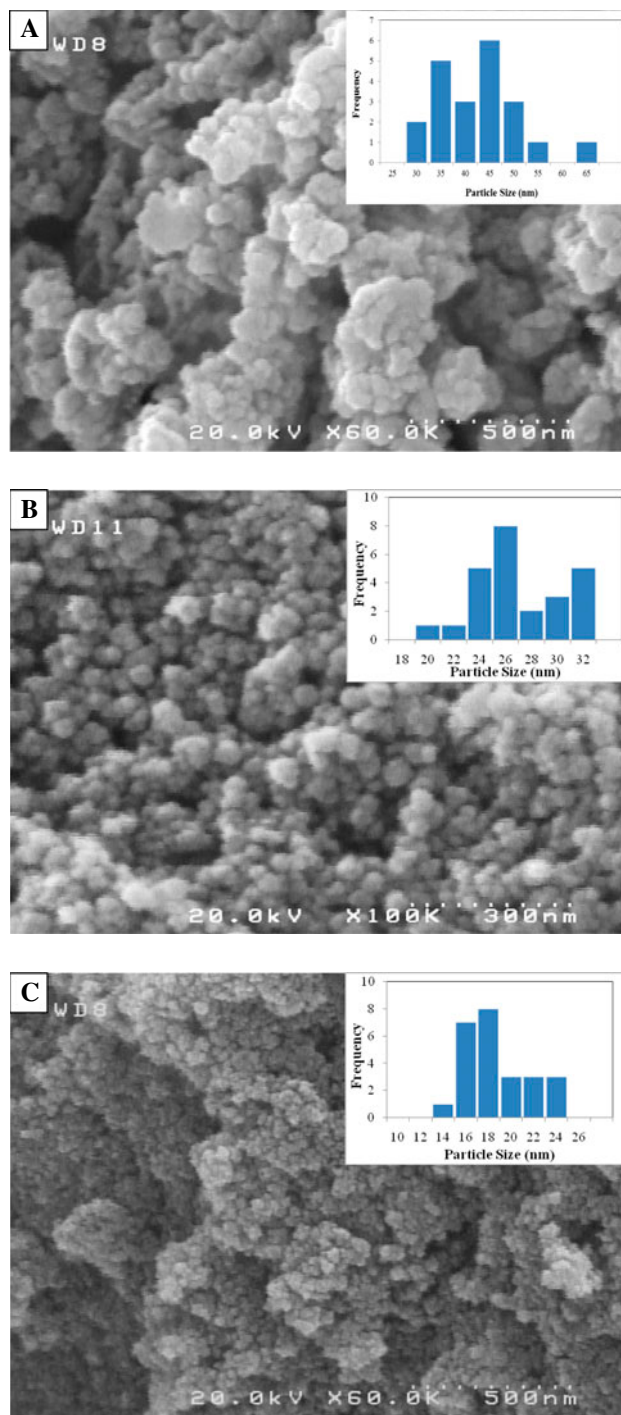


Fig. 4. SEM micrographs for (A) Fe₃O₄-chitosan, (B) Fe₃O₄-chitosan-TPP nanogels, and (C) Fe₃O₄-chitosan-glutaraldehyde nanogels.

processes. To well understand the adsorption mechanism and kinetics, pseudo-first-order [35] and pseudo-second-order model were used to investigate the kinetics of MO adsorption on the three synthesized nanoparticles.

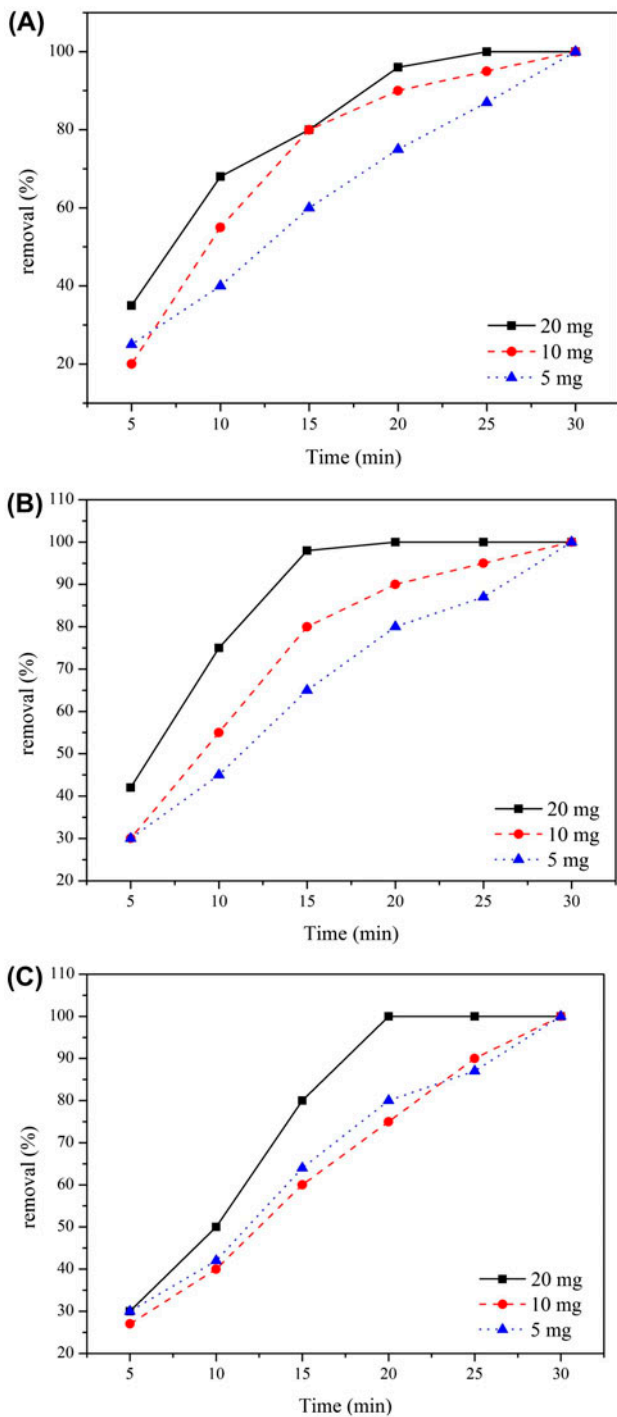


Fig. 5. Effect of amount of adsorbent on adsorption: (A) Fe₃O₄-chitosan, (B) Fe₃O₄-chitosan-TPP nanogels, and (C) Fe₃O₄-chitosan-glutaraldehyde nanogels.

(1) Pseudo-first-order model:

$$\log(q_e - q_t) = \log q_e - (k_1/2.303)t \tag{3}$$

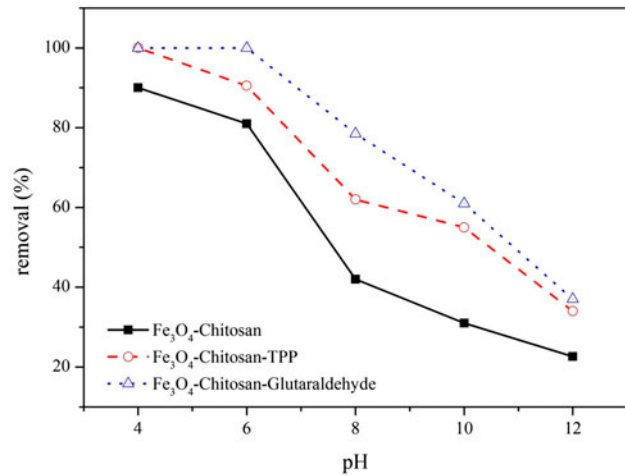


Fig. 6. Effect of pH on adsorption.

(2) Pseudo-second-order model:

$$t/q_t = 1/k_2 q_e^2 + t/q_e \tag{4}$$

where q_e and q_t refer to the amount of MO adsorbed (mg g^{-1}) at equilibrium and at time t (min), k_1 is the overall rate constant of pseudo-first-order reaction (min^{-1}), h is the initial rate constant, k_2 is the overall rate constant of the pseudo-second-order reaction ($\text{g mg}^{-1} \text{min}^{-1}$). Fig. 7(A) and (B) shows the straight line plots of $\log(q_e - q_t)$ vs. t and t/q_t vs. t for different initial dye concentrations. As shown in Fig. 7 (Table 2), the pseudo-first-order curves did not fit well with the experimental data, whereas the pseudo-second-order equation provided an excellent fit for the experimental data with a good linearization of all $R^2 > 0.993$.

3.5. Isotherm study of dye removal

Adsorption isotherms are basic requirements for the design of adsorption systems used for the removal of pollutants. Various isotherm models such as the Langmuir and the Freundlich models were attempted [36,37]. Langmuir isotherm describes that the extent of adsorbate coverage limited to one molecular layer is reached. Langmuir equation can be written as follows:

$$C_e/q_e = 1/(K_L Q_0) + C_e/Q_0 \tag{5}$$

where C_e , K_L , and Q_0 are the equilibrium concentration of dye solution (mg/L), Langmuir constant (L/mg), and the maximum adsorption capacity (mg/g), respectively.

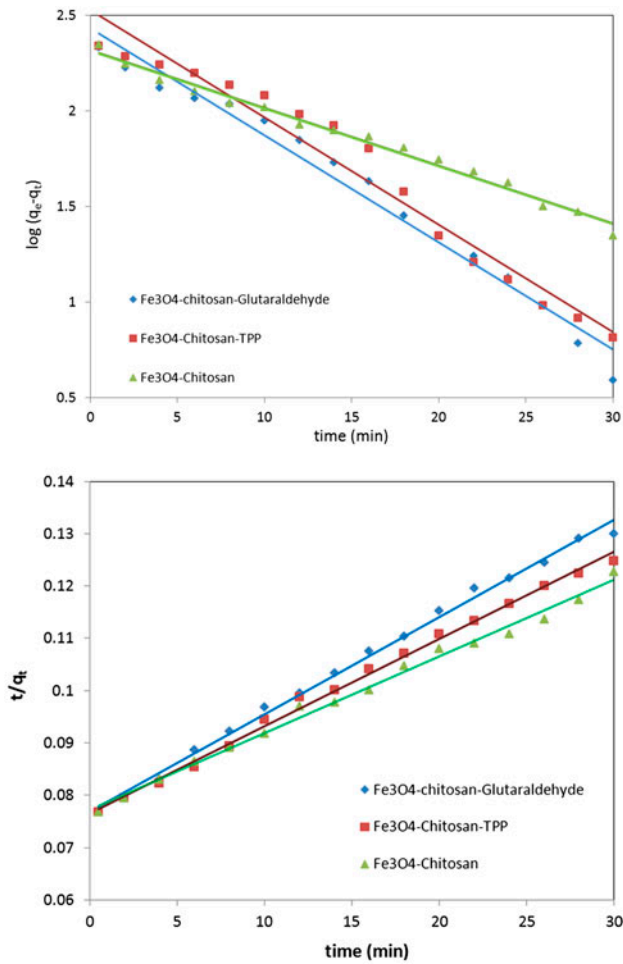


Fig. 7. Plots of $\log(q_e - q_i)$ vs. t (A) and t/q_t vs. t (B) for MO adsorption for three magnetic nanoparticles.

Freundlich isotherm can be expressed by:

$$\log q_e = \log K_F + (1/n) \log C_e \quad (6)$$

where K_F is adsorption capacity at unit concentration (L/g) and $1/n$ is adsorption intensity.

To study the applicability of the Langmuir and the Freundlich isotherms for the dye adsorption, linear

Table 3
Linearized isotherm coefficients for dye adsorption

Langmuir isotherm			Freundlich isotherm		
Q_0	K_L	R^2	K_F	$1/n$	R^2
167	0.3	0.995	47.09	0.556	0.986

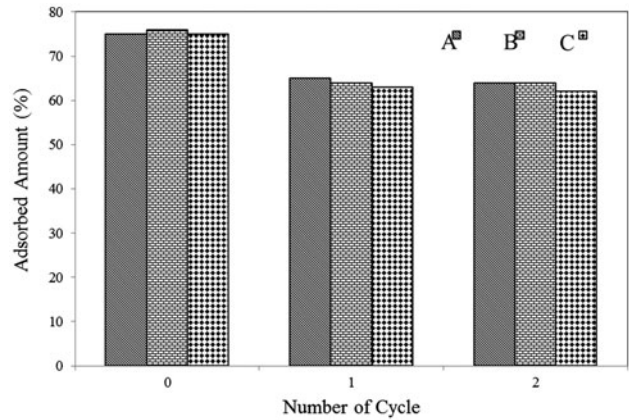


Fig. 8. Regeneration and reusability of (A) Fe_3O_4 -chitosan, (B) Fe_3O_4 -chitosan-TPP nanogels, and (C) Fe_3O_4 -chitosan-glutaraldehyde nanogels.

plots of C_e/q_e against C_e and $\log q_e$ vs. $\log C_e$ are plotted. The values of Q_0 , K_L , K_F , $1/n$, and R^2 (correlation coefficient values of all isotherms models) are shown in Table 3.

3.6. Regeneration/desorption of adsorbent

Regeneration of spent adsorbent is considered as an important economical aspect to minimize the material cost. The saturated three types of nanogels were redispersed in NaOH solution (0.1 M) via shaking with a final concentration of 0.1 g/L. After shaking, the nanogels were separated with an external magnet, and washed with deionized water for three times. Then, the regenerated magnetic adsorbent was redispersed in deionized water for reuse. The adsorption

Table 2
Kinetics constants for dye adsorption

Adsorbent	Pseudo-first-order			Pseudo-second-order		
	K_1 (min^{-1})	q_e (mg/g)	R^2	K_2 (g/(mg min))	q_e (mg/g)	R^2
Fe_3O_4 -chitosan	0.4788	13.69	0.9863	0.1911	20.01	0.9934
Fe_3O_4 -chitosan-TPP nanogels	0.4662	13.25	0.9612	0.1502	20.42	0.9959
Fe_3O_4 -chitosan-glutaraldehyde nanogels	0.4725	13.19	0.9789	0.1724	20.25	0.9958

capacity of the recycled nanogels was assessed in three consecutive cycles (Fig. 8).

4. Conclusion

The research work presented here shows that dissolved dyes can be successfully removed from aqueous solution by adsorption on new low-cost magnetic Fe₃O₄/chitosan nanocomposites. These adsorbents were found to be useful and valuable means for dye removal from wastewater. The nanocomposites were prepared by co-precipitation process using Fe₃O₄ nanoparticles as magnetic material and chitosan as basic adsorbent. The characterizations' results indicated that magnetic Fe₃O₄ nanoparticles have been successfully introduced into the nanocomposite and kept intrinsic magnetic properties. Fe₃O₄-chitosan-glutaraldehyde nanogel adsorbent exhibited faster adsorption rate toward MO compared with other nanocomposites. It could quickly and efficiently remove the dyes under acidic conditions (pH 4) via the electrostatic interactions between MO anions and chitosan. The adsorption kinetics was well described by the pseudo-second-order model. The adsorption capacity was evaluated under the conditions of varied initial pH and adsorbent dosage and the maximum adsorption capacity is about 20.5 mg/g, with good cycling stability of 64% retention of the initial adsorption value after three adsorption/desorption cycles.

Acknowledgments

The authors express gratefulness to the Zanjan University of Medical Sciences and University of Zanjan.

References

- [1] S. Wang, C. Wei, W. Wang, Q. Li, L. Li, A comparative study on the adsorption of acid and reactive dyes on multiwall carbon nanotubes in single and binary dye systems, *J. Chem. Eng.* 57 (2012) 1563–1569.
- [2] H.Y. Zhu, R. Jiang, L. Xiao, W. Li, A novel magnetically separable γ -Fe₂O₃/crosslinked chitosan adsorbent: Preparation, characterization and adsorption application for removal of hazardous azo dye, *J. Hazard. Mater.* 179 (2010) 251–257.
- [3] L. Fan, C. Luo, M. Sun, H. Qiu, X. Li, Synthesis of magnetic β -cyclodextrin-chitosan/graphene oxide as nanoadsorbent and its application in dye adsorption and removal, *Colloids Surf. B: Biointerfaces* 103 (2013) 601–607.
- [4] L. Fan, M. Li, Z. Lv, M. Sun, C. Luo, F. Lu, H. Qiu, Fabrication of magnetic chitosan nanoparticles grafted with β -cyclodextrin as effective adsorbents toward hydroquinol, *Colloids Surf. B: Biointerfaces* 95 (2012) 42–49.
- [5] C.S. Shen, S.F. Song, L.L. Zang, X.D. Kang, Y.Z. Wen, W.P. Liu, L.S. Fu, Efficient removal of dyes in water using chitosan microsphere supported cobalt (II) tetrasulfophthalocyanine with H₂O₂, *J. Hazard. Mater.* 177 (2010) 560–566.
- [6] H.F. Wu, S.H. Wang, H.L. Kong, T.T. Liu, M.F. Xia, Performance of combined process of anoxic baffled reactor-biological contact oxidation treating printing and dyeing wastewater, *Bioresour. Technol.* 98 (2007) 1501–1504.
- [7] G. Muthuraman, Extractive removal of astacryl blue BG and astacryl golden yellow dyes from aqueous solutions by liquid-liquid extraction, *Desalination* 277 (2011) 308–312.
- [8] Y.A. Degs, M.A.M. Khraisheh, S.J. Allen, M.N. Ahmad, Effect of carbon surface chemistry on the removal of reactive dyes from textile effluent, *Water Res.* 34 (2000) 927–935.
- [9] N.A. Travlou, G.Z. Kyzas, N.K. Lazaridis, E.A. Deliyanni, Functionalization of graphite oxide with magnetic chitosan for the preparation of a nanocomposite dye adsorbent, *Langmuir* 29 (2013) 1657–1668.
- [10] Y. Yu, Y.Y. Zhuang, Z.H. Wang, M.Q. Qiu, Adsorption of water-soluble dyes onto resin NKZ, *Ind. Eng. Chem. Res.* 42 (2003) 6898–6903.
- [11] L. Zhou, C. Gao, W. Xu, Magnetic dendritic materials for highly efficient adsorption of dyes and drugs, *ACS Appl. Mater. Interfaces* 2 (2010) 1483–1491.
- [12] C. Shen, Y. Shen, Y. Wen, H. Wang, W. Liu, Fast and highly efficient removal of dyes under alkaline conditions using magnetic chitosan-Fe(III) hydrogel, *Water Res.* 45 (2011) 5200–5210.
- [13] S. Shariati, M. Faraji, Y. Yamini, A.A. Rajabi, Fe₃O₄ magnetic nanoparticles modified with sodium dodecyl sulfate for removal of safranin O dye from aqueous solutions, *Desalination* 270 (2011) 160–165.
- [14] A.P. Zhu, L.H. Yuan, T.Q. Liao, Suspension of Fe₃O₄ nanoparticles stabilized by chitosan and O-carboxymethyl chitosan, *Int. J. Pharm.* 350 (2008) 361–368.
- [15] G.Y. Li, Y.R. Jiang, K.L. Huang, P. Ding, J. Chen, Preparation and properties of magnetic Fe₃O₄-chitosan nanoparticle, *J. Alloys Compd.* 466 (2008) 451–456.
- [16] Y. Wu, Y.J. Wang, G.S. Luo, Y.Y. Dai, In situ preparation of magnetic Fe₃O₄-chitosan nanoparticles for lipase immobilization by cross-linking and oxidation in aqueous solution, *Bioresour. Technol.* 100 (2009) 3459–3464.
- [17] P. Djomgoue, M. Siewe, E. Djoufac, P. Kenfack, D. Njopwouo, Surface modification of Cameroonian magnetite rich clay with Eriochrome Black T. Application for adsorption of nickel in aqueous solution, *Appl. Surf. Sci.* 258 (2012) 7470–7479.
- [18] M. Usman, S. Martin, N. Cimetière, S. Giraudet, V. Chatain, K. Hanna, Sorption of nalidixic acid onto micrometric and nanometric magnetites: Experimental study and modeling, *Appl. Surf. Sci.* 299 (2014) 136–145.
- [19] Y.Y. Xu, M. Zhou, H.J. Geng, J.J. Hao, Q.Q. Ou, S.D. Qi, H.L. Chen, X.G. Chen, A simplified method for synthesis of Fe₃O₄@PAA nanoparticles and its application for the removal of basic dyes, *Appl. Surf. Sci.* 258 (2012) 3897–3902.

- [20] M. Mikhaylova, D.K. Kim, N. Bobrysheva, M. Osmolowsky, V. Semenov, T. Tsakalacos, M. Muhammed, Superparamagnetism of magnetite nanoparticles: Dependence on surface modification, *Langmuir* 20 (2004) 2472–2477.
- [21] Y.F. Lin, H.W. Chen, Y.C. Chen, C.S. Chiou, Application of magnetite modified with polyacrylamide to adsorb phosphate in aqueous solution, *J. Taiwan Inst. Chem. Eng.* 44 (2013) 45–51.
- [22] J.S. Piccin, G.L. Dotto, M.L.G. Vieira, L.A.A. Pinto, Kinetics and mechanism of the food dye FD&C Red 40 adsorption onto chitosan, *J. Chem. Eng.* 56 (2011) 3759–3765.
- [23] Y.C. Chang, D.H. Chen, Preparation and adsorption properties of monodisperse chitosan-bound Fe_3O_4 magnetic nanoparticles for removal of Cu(II) ions, *J. Colloid Interface Sci.* 283 (2005) 446–451.
- [24] G. Zhao, J.J. Xu, H.Y. Chen, Fabrication, characterization of Fe_3O_4 multilayer film and its application in promoting direct electron transfer of hemoglobin, *Electrochem. Commun.* 8 (2006) 148–154.
- [25] M.A. Morales, E.C. de Souza Rodrigues, A.S.C.M. de Amorim, J.M. Soares, F. Galembeck, Size selected synthesis of magnetite nanoparticles in chitosan matrix, *Appl. Surf. Sci.* 275 (2013) 71–74.
- [26] S.K. Giri, N.N. Das, G.C. Pradhan, Synthesis and characterization of magnetite nanoparticles using waste iron ore tailings for adsorptive removal of dyes from aqueous solution, *Colloids Surf. A: Physicochem. Eng. Aspects* 389 (2011) 43–49.
- [27] H.Y. Zhu, R. Jiang, L. Xiao, Adsorption of an anionic azo dye by chitosan/kaolin/ $\gamma\text{-Fe}_2\text{O}_3$ composites, *Appl. Clay Sci.* 48 (2010) 522–526.
- [28] V. Zamora-Mora, M. Fernández-Gutiérrez, J. San Román, G. Goya, R. Hernández, C. Mijangos, Magnetic core-shell chitosan nanoparticles: Rheological characterization and hyperthermia application, *Carbohydr. Polym.* 102 (2014) 691–698.
- [29] S. Sadighian, K. Rostamizadeh, H. Hosseini-Monfared, M. Hamidi, Doxorubicin-conjugated core-shell magnetite nanoparticles as dual-targeting carriers for anticancer drug delivery, *Colloids Surf. B* 117 (2014) 406–413.
- [30] M. Khalkhali, K. Rostamizadeh, S. Sadighian, F. Khoeini, M. Naghibi, M. Hamidi, The impact of polymer coatings on magnetite nanoparticles performance as MRI contrast agents: A comparative study, *DARU J. Pharm. Sci.* 23 (2015) 595.
- [31] G.Z. Kyzas, E.A. Deliyanni, N.K. Lazaridis, Magnetic modification of microporous carbon for dye adsorption, *J. Colloid Interface Sci.* 430 (2014) 166–173.
- [32] J. Qu, G. Liu, Y. Wang, R. Hong, Preparation of Fe_3O_4 -chitosan nanoparticles used for hyperthermia, *Adv. Powder Technol.* 21 (2010) 461–467.
- [33] S. Sadighian, H. Hosseini-Monfared, K. Rostamizadeh, M. Hamidi, pH-triggered magnetic-chitosan nanogels (MCNs) for doxorubicin delivery: Physically vs chemically cross linking approach, *Adv. Pharm. Bull.* 5(1) (2015) 115–120.
- [34] M. Doğan, H. Abak, M. Alkan, Adsorption of methylene blue onto hazelnut shell: Kinetics, mechanism and activation parameters, *J. Hazard. Mater.* 164 (2009) 172–181.
- [35] Y.S. Ho, G. McKay, A comparison of chemisorption kinetic models applied to pollutant removal on various sorbents, *Process Saf. Environ. Prot.* 76 (1998) 332–340.
- [36] I. Langmuir, The constitution and fundamental properties of solids and liquids, *J. Am. Chem. Soc.* 38 (1916) 2221–2295.
- [37] A. Özcan, E.M. Öncü, A.S. Özcan, Kinetics, isotherm and thermodynamic studies of adsorption of Acid Blue 193 from aqueous solutions onto natural sepiolite, *Colloid Surf. A: Physicochem. Eng. Aspects* 277 (2006) 90–97.